Neuderth P., Hille P., Martí-Sánchez S., de la Mata M., Coll M., Arbiol J., Eickhoff M.. Optical Analysis of Oxygen Self-Diffusion in Ultrathin CeO2 Layers at Low Temperatures. Advanced Energy Materials, (2018). 8. 1802120: - . 10.1002/aenm.201802120,

Optical analysis of oxygen self-diffusion in ultra-thin CeO_2 layers at low temperatures

P. Neuderth,*[,ab] P. Hille,[ac] M. Coll[d], S. Martí-Sánchez,[e] M. de la Mata,[e] J. Arbiol,[ef] Martin Eickhoff[ac]

[a]Institute of Experimental Physics I, Justus Liebig University Giessen, 35392 Giessen, Germany.
[b]Center for Materials Research (LaMa), Justus Liebig University Giessen, 35392 Giessen, Germany.
[c]Institute of Solid State Physics, University of Bremen, 28359 Bremen, Germany.
[d]Institut de Ciencia de Materials de Barcelona, ICMAB-CSIC, 08193 Barcelona, Spain.
[e]Catalan Institute of Nanoscience and Nanotechnology (ICN2), CSIC and BIST, 08193 Barcelona, Spain
[f]ICREA, Pg. Lluís Companys 23, 08010 Barcelona, CAT, Spain

**paula.j.neuderth@exp1.physik.uni-giessen.de*

Abstract

An optical in-situ strategy for the analysis of oxygen diffusion in ultra-thin ceria layers with a thickness of 2-10 nm at temperatures between 50 and 200 °C is presented, which allows for the determination of diffusion coefficients. This method is based on the sensitivity of the photoluminescence (PL) intensity of InGaN nanowires to adsorbed oxygen. The oxygen diffusion through an ultra-thin CeO_2 *coating deposited on the InGaN nanowires is monitored by analyzing the transient PL behavior of the InGaN nanowires, which responds to changes of the oxygen concentration in the environment when the corresponding oxygen concentration is established at the* CeO_2*/InGaN interface due to diffusion through the coating. Quantitative evaluation of the oxygen diffusion in* CeO_2 *based on Langmuir Adsorption and Recombination model yields a diffusion coefficient D of* $(3.3 \pm 0.8) \cdot 10^{-16}\ cm^2/s$ *at a temperature of 100 °C. Temperature-dependent measurements reveal an Arrhenius type behavior of D with an activation energy of (0.28 ± 0.08) eV. In contrast, no oxygen diffusion is detected for an ultra-thin layer (≥ 5 nm) of* Al_2O_3*, which is known as a poor oxygen ion conductor within the analyzed temperature regime.*

Introduction

Understanding of the chemical diffusion processes and the knowledge of diffusion coefficients is essential for the design of ion-conducting layers in batteries or catalysts. A material of high interest regarding the diffusion properties of oxygen is CeO_2. It is known to exhibit a high oxygen diffusion coefficient, as oxygen vacancies are easily formed in its fluorite structure, which is the basis of the oxygen diffusion mechanism.[1,2] Typically, CeO_2 is doped with rare earth materials (*e.g.* Y, Nd, Gd, Sm, Pr, La) or transition metal oxides (mainly Zr) to enhance the oxygen storage and diffusion properties.[2-4] In this work we focus on the oxygen diffusion in nominally undoped ultra-thin CeO_2 layers grown by atomic layer deposition (ALD) to gain insight into basic material properties.

Oxygen self-diffusion coefficients in CeO_2 are usually determined by experiments with isotope tracers, like O^{18} in combination with secondary ion mass spectrometry (SIMS)[4-6] or gas phase analysis[5] at elevated temperatures above 1000 K. Alternatively, self-diffusion coefficients are also estimated from conductivity measurements.[2, 4, 7] Reported literature values for the oxygen diffusion coefficient extracted from such methods range between 10^{-12} and 10^{-7} cm^2/s at 1000 K and exhibit activation energies between 0.4 eV and 2.3 eV.[2,5,6,8-10] The wide variation of the reported values mirrors the experimental difficulties involved in the determination of the oxygen self-diffusion coefficient. Furthermore, the methods reported so far are mainly applicable for bulk material. Hence, due to the small diffusion lengths involved, determination of the diffusion coefficients at room temperature or moderate temperatures below 200°C has not been reported.

In this work we present an optical approach for the non-intrusive *in-situ* monitoring of oxygen self-diffusion and the determination of oxygen diffusion coefficients in ultra-thin CeO_2 layers deposited by ALD on InGaN/GaN nanowire heterostructures. The latter serve as optical probes for the photoluminescence (PL) detection of interfacial oxygen adsorption, as their PL intensity is efficiently quenched upon adsorption of oxygen.[11,12] Here, the diffusion of oxygen through the CeO_2 coating, *i.e.* the temporal evolution of the oxygen concentration at the InGaN/CeO_2 interface, is monitored via detection of the time-dependent photoluminescence intensity. Investigation of different layer thicknesses and quantitative modelling of the extracted transients allows for quantitative estimation of the diffusion coefficients. This non-destructive *in-situ* technique is applicable for ultra-thin layers and for temperatures below 200°C.

Results and Discussion

Sample design and concept

InGaN/GaN nanowire structures which feature a PL quenching response upon exposure to oxygen and other oxidizing gases[11,12] were coated with a 2-10 nm thick homogeneous CeO_2 layer by ALD as displayed in the schematic and in the high resolution transmission electron microscopy (HRTEM) image in **Figure 1**.

The PL characteristics of the resulting nanocomposite in atmospheres with different oxygen concentration were recorded at temperatures of 50, 100, 150 and 200 °C. Due to the dense, homogeneous ALD coating, the InGaN core of the nanowire composite was not in direct contact with the surrounding gas atmosphere. To cause a PL quenching response to the oxygen-containing atmosphere, oxygen has to diffuse through the CeO_2 coating until it reaches the CeO_2/InGaN interface. The related time delay was detected in a transient PL measurement in direct comparison with the behavior of an uncoated InGaN/GaN reference. As the CeO_2 coatings show 97% transparence for the PL excitation wavelength of 405 nm (supporting information **S1**) electron hole pairs were almost exclusively photogenerated in the InGaN core.

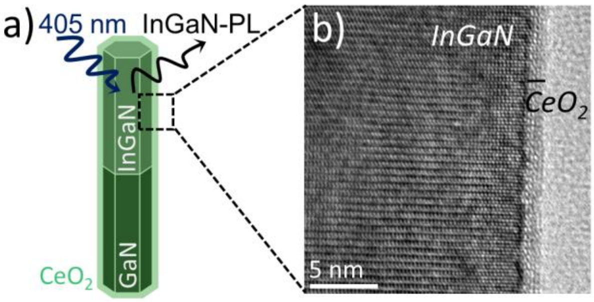

Figure 1. (a) Schematic sample structure with InGaN/GaN core and CeO_2 ALD coating. The InGaN core is excited with a 405 nm laser diode and the InGaN PL is transiently measured. **(b)** Example of HRTEM image with 2 nm CeO_2 coating on the InGaN part of an InGaN/GaN nanowire.

Influence of CeO_2 coatings on the oxygen response of InGaN nanowires

Figure 2a shows PL spectra of uncoated InGaN/GaN nanowires (NWs) for different oxygen concentrations and temperatures. In both cases, an increase of the respective entity results in quenching of the PL with the spectral shape remaining unchanged. In **Figure 2b** similar PL spectra are shown for a 5 nm CeO_2-coated sample. Also in this case, thermal and oxygen-induced quenching is observed, but the relative response to oxygen is reduced. The observation, that oxygen has an influence on the InGaN PL intensity of 5 nm CeO_2 coated samples indicates that oxygen passes the coating and reaches the CeO_2/InGaN interface, were the PL quenching is induced due to interfacial oxygen adsorption.

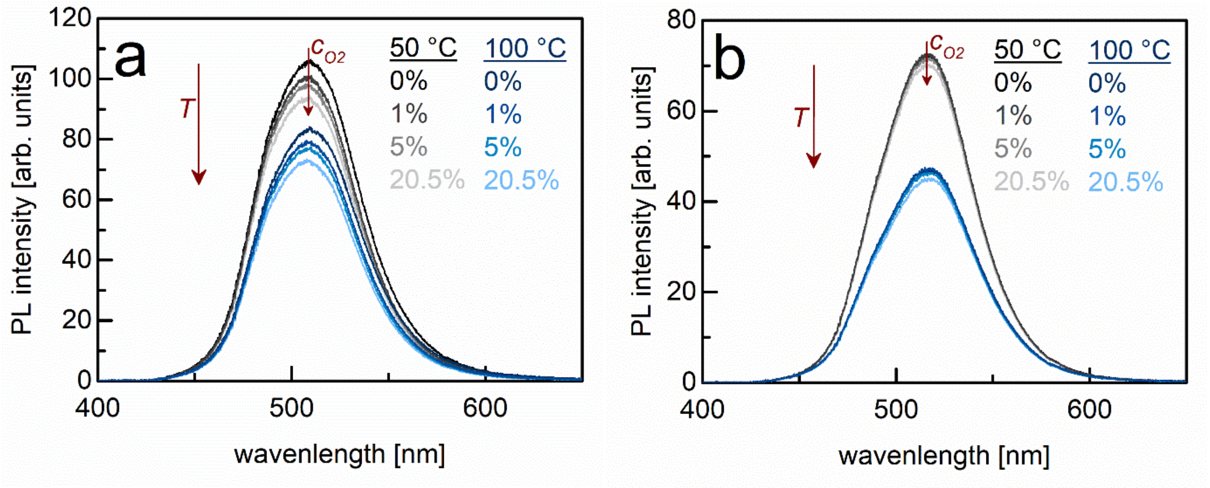

Figure 2. InGaN-PL spectra for different oxygen concentration at 50°C and 100°C; **(a)** uncoated InGaN/GaN NWs; **(b)** 5 nm CeO_2 coated InGaN/GaN NWs.

Oxygen-induced relative PL intensity changes (responses) and their temporal evolution were investigated by a transient collection of PL spectra and evaluation of the PL intensities which were integrated over the spectral range between 400 and 700 nm.

In **Figure 3a** the transient PL response for alternating intervals of pure nitrogen and 20.5% oxygen in nitrogen of the uncoated InGaN/GaN reference (black curve) and hybrid structures with CeO_2 coatings of different thickness (colors indicated in the figure) are compared. A detail of the transient measurements is shown in **Figure 3b,** which displays a magnification of the first 30 s during exposure to oxygen. Here, the transients are normalized to their maximum intensity at the end of the nitrogen interval, *t=0* is the switching point between pure nitrogen and the nitrogen/oxygen mixture (synthetic air).

For the reference sample the typical decrease of the PL intensity in oxygen containing atmosphere, attributed to the enhancement of non-radiative recombination due to oxygen adsorption[11,12], is observed. The magnification in **Figure 3b** shows that the reference sample immediately responds to oxygen, with a response time as fast as the resolution of the transient measurement (below 4 s). In **Figure 3c** (black symbols) the thermal quenching of PL intensity is displayed, whereas in **Fig. 3d** the increase of PL quenching response to oxygen with increasing temperature is depicted. The latter is also mirrored by an increase in adsorption energy with increasing temperature that can be extracted from fits of the response curves according to the Langmuir adsorption-recombination model (LAR model) that has recently been described in Ref. [12].

InGaN/GaN nanowires coated with 2, 5, 10 nm of ceria respectively (colored curves in **Figure 3a**) also show a decrease in PL intensity upon exposure to oxygen that is qualitatively comparable to the uncoated InGaN/GaN nanowires. As the InGaN core is separated from the gas environment by the

CeO_2 coating this result indicates oxygen diffuses through the ceria film and causes quenching of the PL intensity when reaching the InGaN/CeO_2-interface. In the magnified presentation of **Figure 3b**, it is seen that the time delay for the first measurable response to oxygen increases with increasing film thickness. However, similar to the uncoated sample, the sample with the 2 nm CeO_2 coating does not show any time delay and immediately responds to the oxygen exposure.

The PL intensity (**Figure 3c**) and the magnitude of the relative oxygen response (**Figure 3d**) are reduced and systematically decrease with increasing film thickness. The temperature dependence remains qualitatively comparable to that of uncoated nanowires.

In contrast, InGaN/GaN nanowires coated with ultra-thin Al_2O_3 layers do only show a response to oxygen for an Al_2O_3 thickness of 2 nm. This response is qualitatively similar to that of samples coated with 2 nm of CeO_2, but already for a thickness of 5 nm the response of Al_2O_3-coated samples is completely suppressed (cf. insert in **Figure 3a**). As Al_2O_3 is known as a weak oxygen conductor with an oxygen self-diffusion coefficient of $5 \cdot 10^{-17}$ cm^2/s at 1500 °C[13], which is by a factor of 10^{10} smaller than that of CeO_2 ($5 \cdot 10^{-7}$ cm^2/s at 1500 °C; approximated from Ref [5]), the absence of an oxygen response for the sample with the 5 nm coating is due to the fact that the oxygen diffusion proceeds too slow to cause a measurable decrease of the PL intensity at the temperatures applied during the measurements carried out here. This result further supports the interpretation that the delayed oxygen response of CeO_2-coated InGaN nanowires with a coating thickness of 5 – 10 nm indeed corresponds to the oxygen diffusion through the coating material. However, for a 2 nm Al_2O_3 coating a response to oxygen was observed, even though it is not expected due to the small diffusion coefficient. As displayed in **Figure 3b**, the sample with 2 nm Al_2O_3 coating shows an immediate decrease in PL intensity upon oxygen exposure rather than a delayed response, and thus a comparable behavior as the 2 nm CeO_2 and the uncoated samples, indicating that the detection mechanism is different for 2 nm thin coatings and not induced by oxygen diffusion.

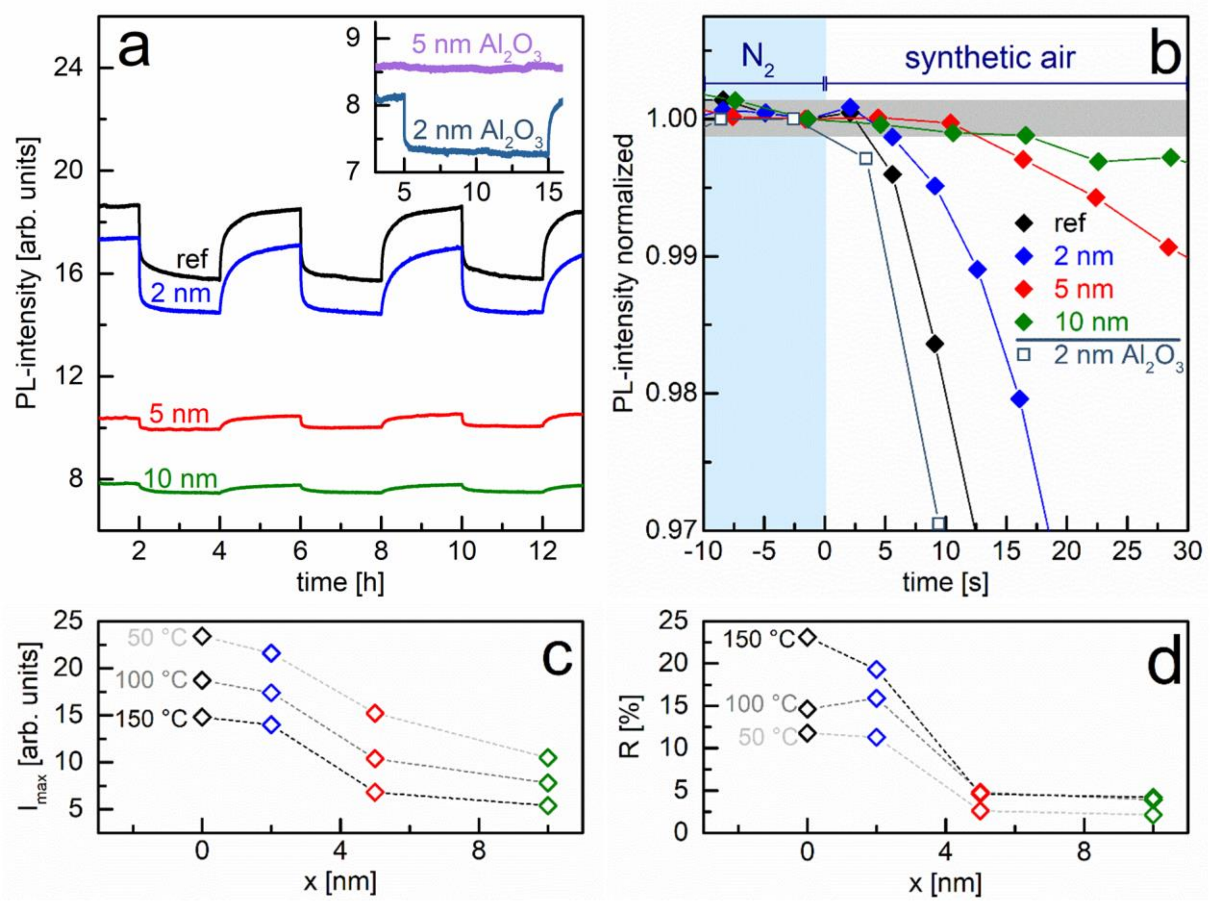

Figure 3. (a) Transient PL intensity measurement of uncoated and 2, 5 and 10 nm CeO_2 coated InGaN nanowires during exposure to alternating 2 h intervals of N_2 and 20.5% O_2 in N_2. Exposure to oxygen leads to a PL quenching. The insert shows a measurement on Al_2O_3 coated samples, with intervals of 5 h. Measurements are at 100 °C. **(b)** Magnification of the transient measurements from Figure (a), the first 30 seconds of the oxygen rich interval are shown. Here, transients are normalized to their maximum intensity at the end of the nitrogen rich interval. t=0 is the switching point between nitrogen and synthetic air. **(c,d)** Extracted data from PL transients of different temperatures and CeO_2 coating thicknesses *x*: **(c)** maximum intensity I_{max} (measured at end of first N_2 interval); **(d)** relative change in PL intensity, R, upon exposure response to oxygen.

Application of the Langmuir-Adsorption-Recombination-Model

To explain the dependence of the PL quenching response of InGaN/GaN NW structures on the oxygen concentration for different temperatures the Langmuir-Adsorption-Recombination-(LAR-)Model was recently introduced by Maier *et al.*[12]. According to that model the maximum oxygen response *R* [%] is given by the maximum relative intensity change induced by a certain oxygen concentration and can be described by formula (1)

$$R[\%] = 100 \cdot (1-PL_{O2}/PL_{N2}), \quad (1)$$

with PL_{N2} being the maximum PL intensity in the nitrogen interval and PL_{O2} being the saturation PL intensity in the oxygen rich interval. According to the LAR model the dependence of the PL response on the surrounding oxygen concentration and temperature is described by formula (2):

$$R = \alpha \cdot \left[\frac{p}{p + p_0 \cdot e^{-\frac{E_{ads}}{k_B T}}} \right] \tag{2}$$

The factor α is the probability for non-radiative surface recombination and depends on molecular properties of the adsorbate, nanowire geometry, temperature and the number of potential adsorption sites. The term in square brackets is the degree of oxygen surface coverage with values between 0 and 1, according to a Langmuir adsorption isotherm. It depends on the oxygen partial pressure p, the thermal energy k_BT and the adsorption energy E_{ads}. p_0 stands for the Langmuir desorption pressure, which is in turn dependent on temperature and the molecular mass of oxygen (for exact expressions see Ref [12]). The LAR model provides a theoretical support for the temperature and concentration dependence of the oxygen response and quantitative results for E_{ads} and α as fitting parameters for the calibration curve in which R is plotted as a function of the oxygen concentration or p. The application of the LAR model to the experimental results discussed here implies that the adsorption behavior can be described by a Langmuir isotherm. This is justified by the assumption that a defined number of oxygen adsorption sites is available at the InGaN/coating interface whose occupation probability between 0 and 1 by diffused oxygen follows the Langmuir isotherm. In that line the oxygen concentration in the solid film can be treated analogue to the partial pressure of a gas atmosphere. As for further evaluation only the interfacial oxygen concentration in saturation is taken into account, the deviation from ideal gas conditions can be overcome.

Quantitative evaluation based on the LAR model was carried out for the response curves of the hybrid nanostructures investigated here. In **Figure 4a-d** the PL response of the uncoated reference and the coated nanowires is shown as a function of the oxygen concentration for different temperatures. The circles in **Figure 4** indicate the experimental data while the solid lines represent the fits according to equation (2).

All curves show the typical S-shape behavior, with zero response at very low concentrations, a quasi-logarithmic increase of response, which covers approximately three orders of magnitude in concentration, and a saturation regime with a maximum response at high concentrations. The concentration, were 50 % of the maximum response is reached (turning point of the curve) is analyte- and temperature-dependent and directly linked to the adsorption energy E_{ads} in the LAR model.

In all cases the fitted curves show good agreement with the experimental data, demonstrating the applicability of the LAR model. The respective saturation levels and the applied oxygen concentration at the turning point of the calibration curves depend on the coating thickness and the measurement temperature.

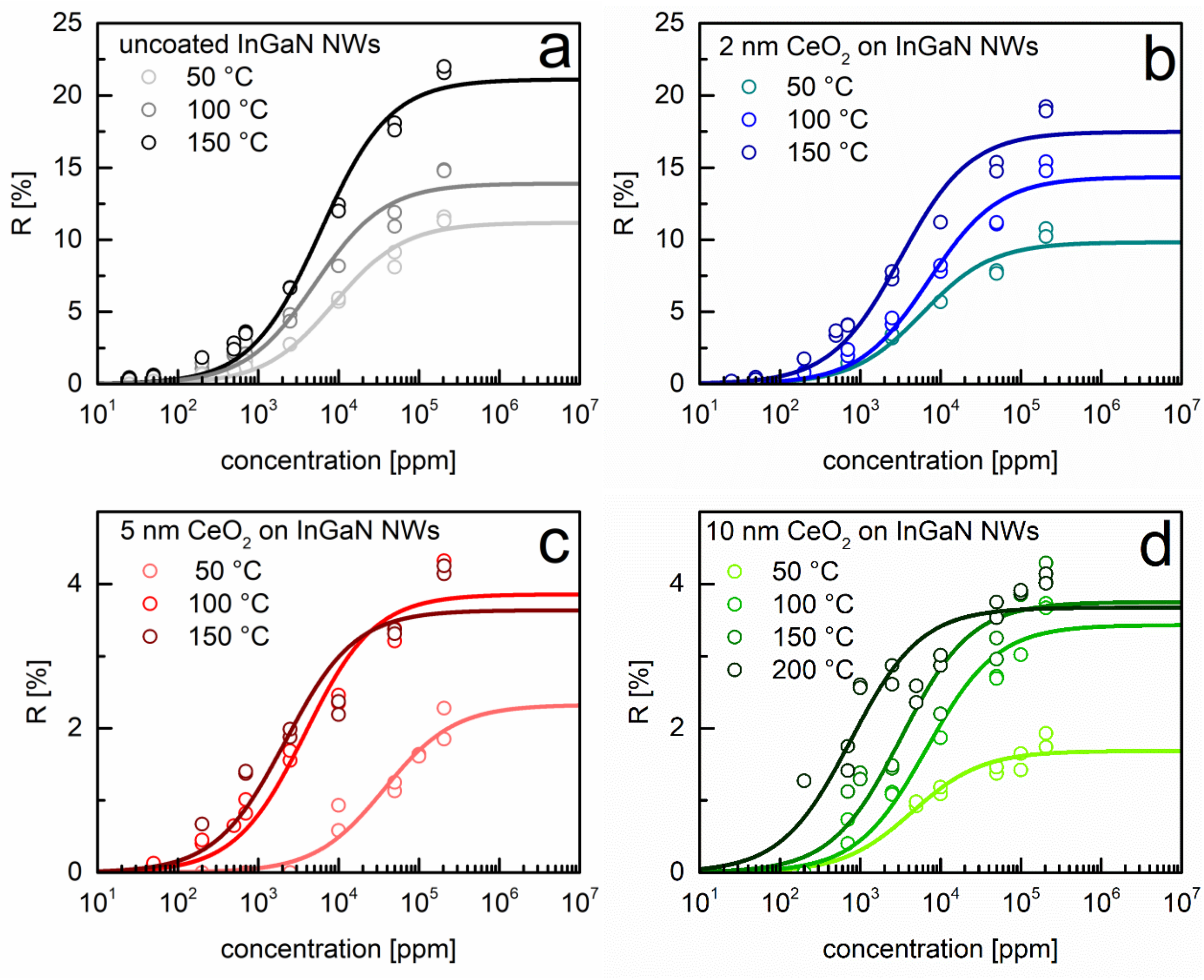

Figure 4. Concentration dependent response measurements fitted by the LAR model **(a)** uncoated, **(b)** 2 nm CeO$_2$-coated, **(c)** 5 nm CeO$_2$-coated and **(d)** 10 nm CeO$_2$-coated. Notice the change in scale of Figure c and d.

The two extracted fitting parameters of the LAR model - the adsorption energy E_{ads} and the non-radiative surface recombination probability α - are displayed as a function of temperature in **Figure 5**. A comparison of these parameters for uncoated and coated samples reveals that the adsorption energy, directly linked to the turning point of the curves, is unaffected by the coating (**Figure 5a**). This indicates that the adsorption process on the natively oxidized InGaN surface and the CeO$_2$ coating exhibits a similar adsorption energy. The latter does not depend on the thickness of the CeO$_2$ film as it is solely determined by the chemical surface properties.

In contrast, the non-radiative surface recombination probability α, mainly given by the response at the saturation level, is reduced for the 5 and 10 nm coated samples, while the values for the 2 nm coating are only slightly reduced compared to the uncoated reference (**Figure 5b**). As α is linked to the number of adsorption sites, this result indicates that the number of adsorption sites at the InGaN/coating interface is reduced compared to an InGaN surface while it is not influenced by the coating thickness. Consequently, full occupation of available adsorption sites is achieved at lower oxygen concentrations.

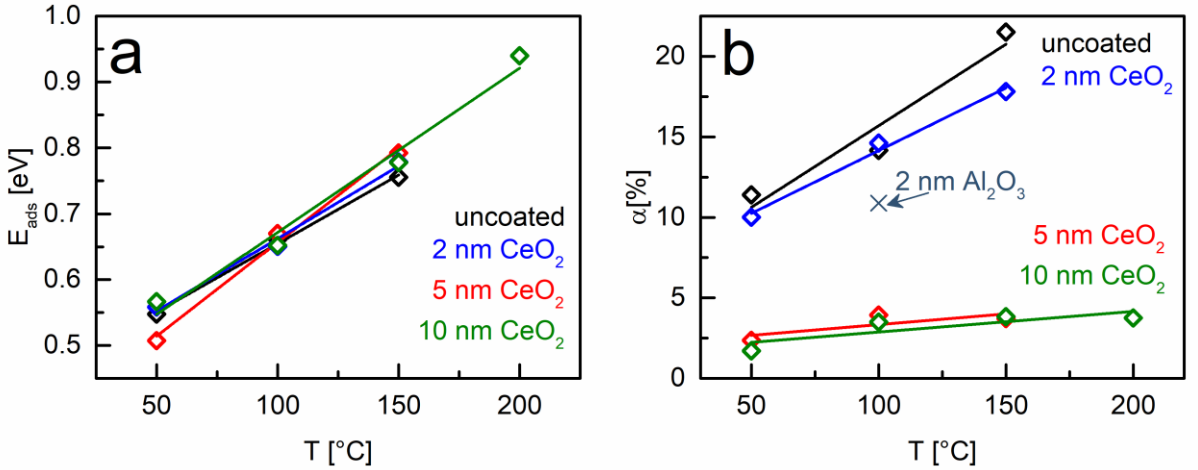

Figure 5. Fit-parameter of LAR-Fits from Figure 3. **(a)** E_{ads} is the adsorption energy, **(b)** α describes the probability of non-radiative surface recombination. The saturation response value of the 2 nm Al_2O_3 coated sample at 100 °C is indicated for comparison.

Determination of diffusion coefficients

Based on the quantitative relation between each PL response value and the respective oxygen concentration provided by the LAR-evaluation, the transient PL response measurements can serve as a base for modelling the oxygen diffusion applying the following strategy (exemplarily shown for a 10 nm CeO_2 coating measured at 150 °C in **Figure 6**):

(1) **Figure 6a** shows the time-dependent response to oxygen obtained by converting the measured *PL(t)* to a *R(t)* curve by equation (1). *t*=0 is the last point of the N_2 interval. The subsequent increase in oxygen response is caused by the exposure to an atmosphere containing 20.5% of oxygen (synthetic air).

(2) The measured response is linked to the oxygen concentration at the InGaN/coating interface by the LAR model. Therefore, the *R(t)* curve can be converted into a curve that displays the temporal evolution of the interfacial oxygen concentration, *c (x=10 nm, t),* represented by the data points in **Figure 6b** (cf. schematic in **Figure 6b**). As α differs for uncoated and differently coated samples, the LAR fit-result for the specific sample and temperature must be used for this conversion.

(3) The *c (x=10 nm, t)* data points in **Figure 6b** are fitted using Fick's second law of diffusion (solid line in **Figure 6b**), expressed in detail in equation (3), if an infinite reservoir of oxygen with a fixed surface concentration c_S is assumed.

$$c(x,t) = c_s \cdot \left[1 - \operatorname{erf}\left(\frac{x}{2\sqrt{Dt}} \right) \right] \tag{3}$$

Here, x is the penetration depth and given by the thickness of CeO_2 coating, c_s is given by the offered oxygen concentration of 0.205 (synthetic air). Therefore, a fit of the $c(x,t)$ curve by equation (3) provides the diffusion coefficient D as fitting parameter.

This fitting procedure is applicable only for those samples where the time delay in the PL response is dominated by the diffusion process. For those samples with a fast PL response, the response time is determined by the exchange of the gas volume in the measurement chamber and hence a fit based in the law of diffusion is not meaningful (cf. supplemental information S2).

In the example of **Figure 6** a diffusion coefficient of $D = 4.4 \cdot 10^{-16}\ cm^2/s$ is obtained for a 10 nm CeO_2-coated sample at a temperature of 150 °C.

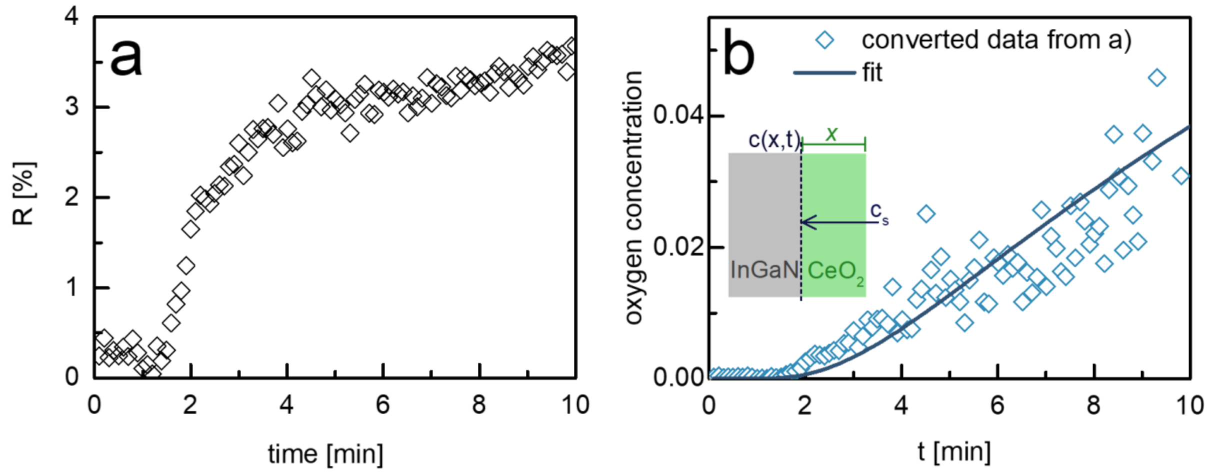

Figure 6. Example for the determination of the diffusion coefficient D: 10 nm CeO_2-coated sample measured at 150 °C. **(a)** Time dependent response to oxygen obtained from measured *PL(t)* curve; t=0 is the beginning of the oxygen rich (20,5% O_2) interval; **(b)** the insert shows schematic of the diffusion process and relevant parameters. c_S is the surface concentration, x is the film thickness and $c(x,t)$ is the oxygen concentration at the InGaN/CeO_2 interface. Data points show the time dependent concentration change at the InGaN/coating interface and are gained from conversion of *R(t)* curve of Figure a) using the LAR-Fit; the solid line shows the fit of the data by Fick's second law (equation (3)) with diffusion coefficient as fitting parameter.

Following this procedure, diffusion coefficients for coatings with a thickness of 5 and 10 nm at temperatures of 50, 100, 150 and 200°C were determined and are displayed in an Arrhenius plot in **Figure 7.** For comparison values for higher temperatures that are reported in literature are also shown. It is evident from the insert in **Figure 7** that the 5 and 10 nm coated samples show similar diffusion coefficients independent of the film thickness, which increase with increasing temperature in an Arrhenius type behavior. A linear fit of these results is indicated in **Figure 7** and reveals an activation energy of E_{act}= (0.28 ± 0.08) eV.

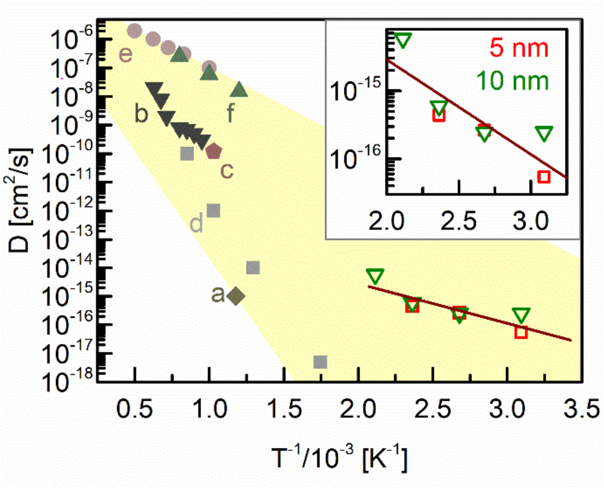

Figure 7. Diffusion coefficients *D*, determined from measurements of 5 and 10 nm CeO_2 coated samples (open symbols). The red line indicates a linear fit. Literature values are shown for comparison in solid symbols: *a-c* determined by O^{18}-tracers and SIMS[8,5,6], *d* determined by conductivity measurements[2] and *e,f* theoretical values for reduced ceria from molecular dynamics simulations. *e* considers $CeO_{1.95}$[9] and *f* considers $CeO_{1.88}$[10]. Yellow area indicates the range which is covered by the approximation of the literature values to the investigated low temperature regime. Insert shows magnification of obtained results and linear fit.

The comparison to existing literature values for the diffusion coefficient *D*, derived from different experimental and theoretical methods, indicated by the solid symbols in **Figure 7**,[2, 5, 6, 8-10] shows that our results fit into the range which is covered by the extrapolation of to the investigated temperature regime of 50-200 °C, as indicated by yellow area in **Figure 7.** Experimental values do only exist for elevated temperatures above 500 °C and were obtained for bulk material.

The related activation energies for the self-diffusion process can be assigned to two diffusion mechanisms, as suggested by Kamiya *et al.*[5]. High activation energies between 1.6 and 2.3 eV[2,5] are attributed to the formation of vacancies which occurs at elevated temperatures above 1000 K[5] and gives rise to an intrinsic diffusion mechanism. Smaller activation energies between 0.4 and 0.6 eV are typically assigned to extrinsic diffusion processes observed for non-stoichiometric ceria already at lower temperatures.[5,9,10] This extrinsic diffusion process is dominated by impurity or defect diffusion, mainly assigned to the oxygen vacancy. These lower activation energies are similar to those obtained for Y- or Gd- doped CeO_2[5] which supports the assumption that the diffusion process observed in this work is impurity-dominated.[5] The activation energy of $E_{act} = 0.28$ eV extracted from our experiments agrees well with the values for extrinsic diffusion, as it is expected for the comparatively high density of oxygen vacancies due to high surface area and small film thickness. Also, a high density of structural defects, like grain boundaries, can result in an enhanced vacancy concentration.

Due to the fast response time an extraction of the diffusion coefficients for the samples with an Al_2O_3-or CeO_2-coating thickness of 2 nm is not possible based on the existing experimental data.

According to **Figures 3** and **4** those samples show an almost instantaneous oxygen response with a similar magnitude, *id est* no time delay due to oxygen diffusion processes is observed for uncoated, 2 nm CeO_2 and 2 nm Al_2O_3 coated samples. In combination with the different extracted α parameter in comparison to the samples with a thicker coating, shown in **Figure 5b**, it can be concluded that a different detection mechanism has to be taken into account for samples with a coating thickness of 2 nm. In particular, oxygen diffusion does not determine PL response time for a coating thickness of 2 nm. The similarity of the extracted α-values and its temperature dependence for the samples with a 2 nm CeO_2 or Al_2O_3 coating and the reference points towards a similar detection mechanism for those samples, particularly as oxygen diffusion is not likely to occur in Al_2O_3.

A possible reason for the observed response characteristics of those structures could be that non radiative recombination via oxygen atoms adsorbed at the surface that occurs via tunneling of photoexcited carriers through the oxide coating rather than the diffusion of oxygen determines the recombination process. The probability of this process is enhanced by the small oxide thickness and possibly further increased by monolayer thickness fluctuations. The strong temperature dependence of this process that rapidly decreases in probability for increasing coating thickness further supports this assignment.

Conclusions

We have presented a strategy for the *in-situ* optical analysis of oxygen diffusion in ultra-thin CeO_2 films with a thickness from 2-10 nm that were deposited on InGaN nanowires by ALD. Employing the sensitivity of the InGaN nanowire photoluminescence to the adsorption of oxygen, diffusion coefficients in the low temperature regime between 50°C and 200 °C could be determined. A quantitative evaluation of PL transients upon exposure of the InGaN/CeO_2 hybrid nanostructures to oxygen was performed using a Langmuir Adsorption and Recombination model in combination with Fick's second law of diffusion. The extracted diffusion coefficients of $5 \cdot 10^{-17}$ to $5 \cdot 10^{-15}$ cm^2/s in the investigated temperature regime (50-200 °C) increase with increasing temperature, exhibiting an activation energy of (0.28 ± 0.08) eV, suggesting a dominant role of extrinsic impurities such as an initially high concentration of oxygen vacancies in the diffusion process. Although literature values in the investigated temperature regime are not available, the extension of reported data to low temperature regime agrees well with the results presented here.

Comparative analysis of Al_2O_3 as a poor oxygen conductor resulted in non-measurable oxygen diffusion down to a thickness of 5 nm. The high and fast oxygen response for CeO_2 and Al_2O_3 coatings with a thickness of 2 nm indicated that for those layer thicknesses the observed oxygen response is not due to oxygen diffusion through the coating but seems to be caused by tunneling of photoexcited carriers to the oxygen adsorbate.

An extension of the proposed method to other oxygen ion conducting materials would allow for systematic analysis of diffusion processes and stabilization mechanisms in ultra-thin layers and their dependence on incorporated defects and impurities.

Experimental

MBE growth of InGaN/GaN nanowires

The InGaN/GaN nanowire core of the nanohybrid structure was prepared by a self-assembled growth process using plasma-assisted molecular beam epitaxy[14] and consists of a GaN base with a height of 390 nm (730 nm for Al_2O_3-coated samples) and an InGaN top part with a height of 350 nm (370 nm for Al_2O_3 coated), the diameter varies between 50 and 100 nm over the substrate area. The position of InGaN PL emission indicates a band gap of approx. 2.4 eV (Al_2O_3-coated: 2.25 eV) at room temperature. From this values the indium content in the alloy was estimated to x= 0.28 for the TiO_2-coated and 0.33 eV for the Al_2O_3-coated samples by taking the literature values E_{GaN}=3.44 eV, E_{InN}=0.76 and b = 1.4 eV [15] into account.

Atomic layer deposition of oxide films

After growth the nanowires were coated with thin films of CeO_2 using atomic layer deposition (ALD). The initial nanowire sample was cut in four pieces, were one piece remained uncoated as reference sample and the other three were coated with 2, 5 and 10 nm ceria film respectively.

ALD of CeO_2 was carried out at a deposition temperature of 270 °C[16] using Ce(thd)$_4$ and ozone as precursors at a deposition rate of 80 cycles per nanometer (thicknesses verified by HRTEM). The film is transparent for the excitation wavelength (405 nm) and PL emission wavelength of InGaN (517 nm). Optical transmission measurements are shown in **Figure S1** of the supplemental information.

Al_2O_3 coatings were prepared by thermal ALD at a growth temperature of 250 °C using trimethylaluminium (TMA) and water as precursors and a deposition rate of 11 cycles per nanometer. The film thicknesses were verified by HRTEM.

Transmission electron microscopy

High resolution transmission electron microscopy (HRTEM) was performed using a TECNAI F20 field emission gun microscope operated at 200 kV with a point to point resolution of 0.14 nm.

Transient photoluminescence measurements

For the PL measurements in atmosphere with controlled oxygen content the sample was mounted in a cell with a continuous gas flow of 200 sccm. A defined mixture of nitrogen and oxygen gas was lead through the chamber; the oxygen concentration was controlled by mass flow controllers.

Temperature control between room temperature and 200 °C was possible by positioning the sample on top of an heated copper block.

For photo excitation of the InGaN the light of a 405 nm laser diode was fiber-coupled through a quartz glass window on top of the chamber. The laser power on the sample was measured with a powermeter and is 29 mW, the spot size on the sample has a diameter of approximately 2 mm. For the photoluminescence measurement the light emitted by the nanowire was fiber-coupled into a QWave USB spectrometer from *rgb lasersystems*. Two pass filters at 435 nm and 425 nm in the detection path were used to cut off the laser wavelength. For recording of the photoluminescence transients the intensity of the PL spectrum was integrated in the wavelength interval between 400 nm - 700 nm with a temporal resolution of 4 seconds.

Acknowledgements

SMS acknowledges funding from "Programa Internacional de Becas "la Caixa"-Severo Ochoa"

ICN2 members acknowledge funding from Generalitat de Catalunya 2017 SGR 327 and the Spanish MINECO project ENE2017-85087-C3. ICN2 acknowledges support from the Severo Ochoa Programme (MINECO, Grant no. SEV-2013-0295) and is funded by the CERCA Programme / Generalitat de Catalunya. Part of the present work has been performed in the framework of Universitat Autònoma de Barcelona Materials Science PhD program. This work has received funding from the European Union's Horizon 2020 Research and Innovation Programme under grant agreement No. 654360 NFFA-Europe. ICN2 and ICIQ acknowledge funding from the BIST Ignite project InWOC2.

References

[1] A. Trovarelli, *Catalysis Reviews: Science and Engineering,* 1996, **38**(4), 439-520.

[2] A. Trovarelli, M. Boaro, E. Rocchini, C. de Leitenburg and G. Dolcetti, *Journal of Alloys and Compounds*, 2001, **323–324**, 584–591.

[3] M. Kamiya, E. Shimada, Y. Ikuma, M. Komatsu and Ha. Haneda, S. Sameshima and Y. Hirata, *J. Mater. Res.*, 2001, **16(**1), 179-184.

[4] E. Ruiz-Trejo, J. D. Sirmana, Yu. M. Baikovb and J. A. Kilner. *Solid State Ionics*, 1998, **113-115**, 565–569

[5] M. Kamiya, E. Shimada, Y. Ikuma, M. Komatsu and H. Haneda, *Journal of The Electrochemical Society*, 2000, **147**(3), 1222-1227.

[6] N. Knoblauch, L. Dörrer, P. Fielitz, M. Schmücker and G. Borchardt, *Phys. Chem. Chem. Phys.,* 2015, **17**, 5849.

[7] G. Chiodelli, G. Flor and M. Scagliotti, *Solid State Ionics*, 1996, **91**, 109-121.

[8] S. Swaroop, M. Kilo, A. Eden Kossoy, I. Lubomirsky and I. Riess, *Solid State Ionics*, 2008, **179**, 1205–1208.

[9] Z. Cui, Y. Sun, J. Qu, *Solid State Ionics*, 2012, **226**, 24–29.

[10] A. Gotte, D. Spångberg, K. Hermansson and M. Baudin, *Solid State Ionics*, 2007, **178**, 1421–1427.

[11] J. Teubert, P. Becker, F. Furtmayr and M. Eickhoff*, Nanotechnology*, 2011, **22**, 275505.

[12] K. Maier, A. Helwig, G. Müller, P. Becker, P. Hille, J. Schörmann, J. Teubert, M. Eickhoff*, Sensors and Actuators B,* 2014, **197**, 87–94.

[13] D. Prot and C. Monty, *Philosophical Magazine A*, 1996, **73**(4), 899-917.

[14] J. Wallys, S. Hoffmann, F. Furtmayr, J. Teubert and M. Eickhoff, *Nanotechnology*, 2012, **23**, 165701.

[15] I. Vurgaftman, J. R. Meyer, *J. Appl. Phys.,* 2003, **94**(6), 3675.

[16] M. Coll, J. Gazquez, A. Palau, M. Varela, X. Obradors and T. Puig, *Chem. Mater*., 2012, **24**, 3732.

Supplemental

S1. Transmission of 5 nm CeO_2 film

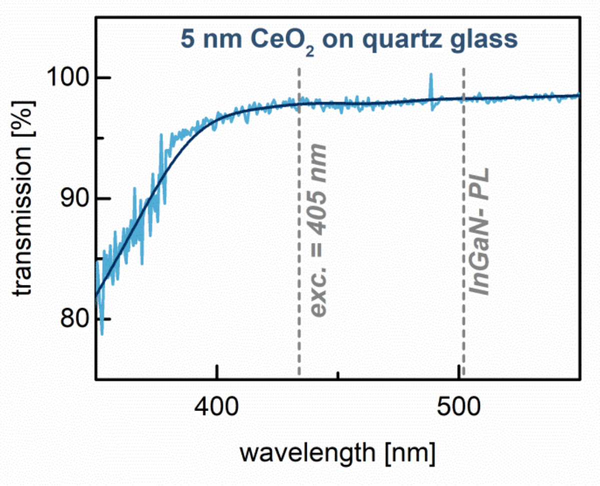

Figure S1. Transmission measurement of a 5 nm CeO_2 film, which was atomic layer deposited on quartz glass. Dotted grey lines indicate the excitation and emission wavelength of the InGaN PL. The film is almost transparent (97%) for both.

S2. Comparison of data and fit

Figure S2 shows a comparison of experimental and theoretical *c(t)* diagrams. Whereas the time-dependent concentration changes of the 5 and 10 nm CeO_2 coated samples are well described by the fits with Fick's second law (solid lines in **Figure S2**), the 2 nm coated sample does not follow the theoretical curve shape. In this case the experimental data follows a qualitatively similar shape as that of the uncoated reference sample.

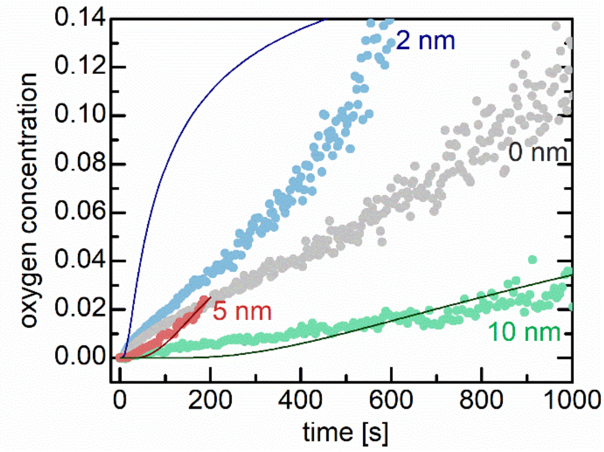

Figure S2. Comparison of measured (dots) and theoretical (solid lines) *c(t)* at 100 °C. For the theoretical curves x=film thickness and D=2.6· 10^{-16} cm^2/s are assumed; The measured values for 5 nm and 10 nm CeO_2-coated samples are in good agreement with the theoretical curve; the 2 nm CeO_2 coated sample does not follow the expected curve shape and shows a comparable behavior to the uncoated reference sample instead.